# Partial reversal of Rett Syndrome-like symptoms in MeCP2 mutant mice

Daniela Tropea[a,1], Emanuela Giacometti[b,1], Nathan R. Wilson[a,1], Caroline Beard[b], Cortina McCurry[a], Dong Dong Fu[b], Ruth Flannery[b], Rudolf Jaenisch[b,c,2], and Mriganka Sur[a,2]

[a]Picower Institute for Learning and Memory and Department of Brain and Cognitive Sciences, Massachusetts Institute of Technology, Cambridge, MA 02139; [b]Whitehead Institute for Biomedical Research, Cambridge, MA 02142; and [c]Department of Biology, Massachusetts Institute of Technology, Cambridge, MA 02139

Contributed by Rudolf Jaenisch, December 11, 2008 (sent for review November 9, 2008)

**Rett Syndrome (RTT) is a severe form of X-linked mental retardation caused by mutations in the gene coding for methyl CpG-binding protein 2 (MECP2). Mice deficient in MeCP2 have a range of physiological and neurological abnormalities that mimic the human syndrome. Here we show that systemic treatment of MeCP2 mutant mice with an active peptide fragment of Insulin-like Growth Factor 1 (IGF-1) extends the life span of the mice, improves locomotor function, ameliorates breathing patterns, and reduces irregularity in heart rate. In addition, treatment with IGF-1 peptide increases brain weight of the mutant mice. Multiple measurements support the hypothesis that RTT results from a deficit in synaptic maturation in the brain: MeCP2 mutant mice have sparse dendritic spines and reduced PSD-95 in motor cortex pyramidal neurons, reduced synaptic amplitude in the same neurons, and protracted cortical plasticity in vivo. Treatment with IGF-1 peptide partially restores spine density and synaptic amplitude, increases PSD-95, and stabilizes cortical plasticity to wild-type levels. Our results thus strongly suggest IGF-1 as a candidate for pharmacological treatment of RTT and potentially of other CNS disorders caused by delayed synapse maturation.**

IGF-1 | plasticity | autism | brain | synapse

Rett Syndrome (RTT) is an X-linked neurological disorder that affects approximately 1 in 10,000 live female births (1). The disorder is characterized by seemingly normal postnatal development followed by a sudden deceleration in growth associated with progressive loss of acquired motor and language skills, stereotypic hand movements, muscle hypotonia, autonomic dysfunctions and severe cognitive impairment. There is no specific treatment for RTT and management is mainly symptomatic and individualized.

In approximately 85% of patients suffering from RTT, the cause is a mutation in the gene coding for methyl CpG-binding protein 2 (MECP2) (2), a global transcriptional modulator (3, 4) that is strongly expressed in the CNS on a time course that correlates with neuronal maturation and synaptogenesis (5). CNS-specific deletion of MeCP2 in mouse models is sufficient to cause Rett-like symptoms (6–8), and activation of the MeCP2 protein even at late stages of the disease can rescue the mutant phenotype (9, 10). An important feature of RTT suggested by mouse models therefore is that it is reversible—the CNS circuits involved apparently do not atrophy but rather remain in a labile, immature state (11), inducing maturation subsequently can repair the syndrome's consequences. Clinical observations have suggested RTT as a genetic disorder of synapse development (12), a feature consistent with findings that cortical and hippocampal brain circuits in MeCP2 mutant mice are characterized by reduced excitatory synaptic drive and synapse number (13, 14).

While MeCP2 target genes have been difficult to identify (15) the best characterized target of MeCP2 regulation is BDNF (16), which is generally known to trigger neuronal and synaptic maturation (17). Overexpression of BDNF indeed restores locomotor activity levels in MeCP2 mutant mice and relieves some symptoms of the mutant phenotype (18). Furthermore, reduced BDNF expression in the brainstem correlates with respiratory dysfunction in MeCP2 mutant mice, and enhancing BDNF expression ameliorates respiratory symptoms (19). Unfortunately, the therapeutic utility of BDNF is hampered by its poor efficiency at crossing the blood–brain barrier. Nevertheless, a therapeutic intervention in humans might thus arise from identifying an agent similarly capable of stimulating synaptic maturation.

A second pleiotrophic growth factor with promise in CNS therapy is Insulin-like Growth Factor 1 (IGF-1). Like BDNF, IGF-1 is widely expressed in the CNS during normal development (20), strongly promotes neuronal cell survival and synaptic maturation (20, 21), and facilitates the maturation of functional plasticity in the developing cortex (22). While BDNF stimulates synaptic strengthening via a pathway involving PI3K/pAkt/PSD-95 (23) and MAPK signaling (17), IGF-1 stimulates the same pathways (22, 24) and has been shown to elevate excitatory postsynaptic currents significantly (25). The biological action of IGF-1 is also regulated by the binding of IGF binding proteins (IGFBP1–6), which may be of significance to RTT and other disorders. IGFBP3, for example, has a binding site for the MeCP2 protein (26), and MeCP2 null mice and RTT patients express aberrantly high levels of IGFBP3 (27), which can be expected in turn to inhibit IGF-1 signaling. Depressed IGF-1 signaling has indeed been implicated in autism spectrum disorder (28).

Unlike BDNF, IGF-1 is capable of crossing the blood–brain barrier, particularly in its tri-peptide form (1–3)IGF-1 (29), where it retains strong neurotrophic efficacy (22, 30, 31). IGF-1 signaling thus offers an attractive target for engaging key molecular pathways to potentially stimulate synaptic maturation and reverse the RTT phenotype, in a format that is more amenable to therapeutic administration to RTT patients. We therefore investigated the potential of (1–3)IGF-1, delivered systemically, to overcome the synaptic and neuronal immaturities that are characteristic of RTT physiopathology (12, 32) and ameliorate RTT-like symptoms in a mouse model of the disorder.

## Results

**(1–3)IGF-1 Administration Increases Lifespan and Improves Locomotor, Respiratory, and Cardiac Function in MeCP2 Mutant Mice.** To test whether (1–3)IGF-1 treatment would impact the development of cardinal features of RTT, we treated MeCP2 -/y mice (6) with daily intraperitoneal injections of the drug starting at roughly 2 weeks of age (see *Materials and Methods*). Compared to vehicle-

Author contributions: D.T., E.G., N.R.W., and M.S. designed research; D.T., E.G., N.R.W., C.B., C.M., D.D.F., and R.F. performed research; R.J. and M.S. contributed new reagents/analytic tools; D.T. and N.R.W. analyzed data; and D.T., E.G., N.R.W., R.J., and M.S. wrote the paper.

The authors declare no conflict of interest.

[1]D.T., E.G., and N.R.W. contributed equally to this work.

[2]To whom correspondence may be addressed. E-mail: jaenisch@wi.mit.edu or msur@mit.edu.

This article contains supporting information online at www.pnas.org/cgi/content/full/0812394106/DCSupplemental.

© 2009 by The National Academy of Sciences of the USA

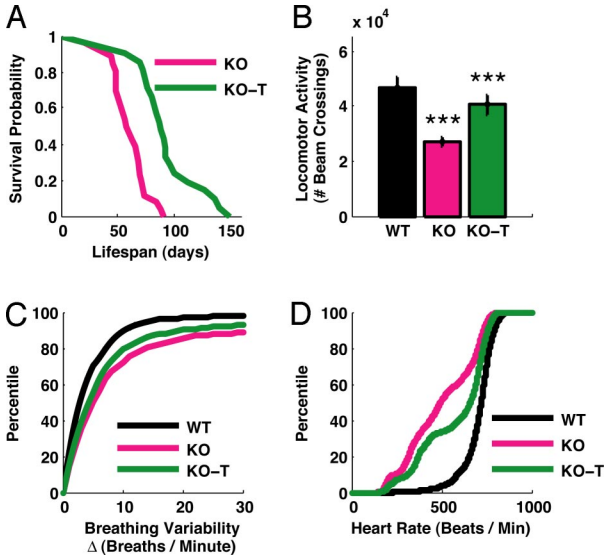


**Fig. 1.** Changes in organismal physiology in MeCP2 mutant mice and the effects of IGF-1 treatment. (*A*) Lifespan as measured by Kaplan-Meier survival curves, showing the proportion of mice that survived (*y* axis) at each day after birth (*x* axis) for nontreated (KO) and treated (KO-T) mice. MeCP2 knockout mice treated with (1–3)IGF-1 daily from P15 onward exhibited a significantly longer life expectancy that their littermates (KO, $n = 26$ mice; KO-T, $n = 21$ mice; $P < 0.00001$, log rank test). (*B*) Locomotor function, measured by placing animals in cages equipped with infrared beams to quantify nocturnal movement. The *y* axis shows the number of beam crossings over 10 h in mice aged 8–9 weeks. Compared to wild-type (WT), MeCP2 knockout mice (KO) showed significantly less activity. However, KO mice treated with (1–3)IGF-1 from P15 onward (KO-T) were more active than vehicle-treated KO animals (WT, 46786 ± 15601 beam crossings, $n = 17$ mice; KO, 27215 ± 6893 crossings, $n = 17$ mice; KO-T, 40455 ± 21592 crossings, $n = 39$ mice; WT vs. KO $P < 0.00001$; KO vs. KO-T $P < 0.001$, 2-tailed *t* test). ***: $P < 0.001$. (*C*) Breathing variability, assessed by measuring breaths per minute with an oximeter and quantifying the change from one measurement interval (15 seconds) to the next. Comparisons are between 8-week-old mice. MeCP2 KO mice showed increased breathing variability (larger changes per interval) than wild-type littermates (WT, 6.0 ± 0.6 breaths/minute, 630 measurements, $n = 13$ mice; KO, 15.4 ± 1.1 breaths/minute, 975 measurements, $n = 17$ mice; $P < 0.00001$, Kolmogorov-Smirnov test). KO-T mice, treated from P15 for 6 weeks, showed decreased variability (smaller changes per interval) than KO (KO-T, 12.3 ± 0.8 breaths/minute, 1292 measurements, $n = 24$ mice; KO-T vs. KO $P < 0.01$, Kolmogorov-Smirnov test). (*D*) Pooled heart rate distributions observed across mice from different treatments (in beats per minute). Comparisons are between 8-week-old mice (WT, KO, and animals which received (1–3)IGF-1 treatment from P:15 for 6 weeks, KO-T). The KO distribution (pink) was left-shifted compared to the wild-type distribution (black), indicating a significant reduction in the distribution of heart rates (WT, $n = 114347$ samples, $n = 5$ mice; KO, 198021 samples, $n = 5$ mice; $P < 0.00001$, Kolmogorov-Smirnov test). The KO-T distribution (green) was in-between the two curves (KO-T, 241251 samples, $n = 9$ mice; KO-T vs. KO $P < 0.00001$, Kolmogorov-Smirnov test), indicating a partial rescue of the KO phenotype toward a more normal wild-type distribution.

treated MeCP2 -/y littermates (KO), MeCP2 -/y mice treated with (1–3)IGF-1 (KO-T) showed an approximately 50% increase in life expectancy (an increase in the 0.5 probability survival rate from approximately 60 days to approximately 90 days), corresponding to a significant enhancement of survival (Fig. 1*A*).

The progressive lethargy associated with RTT prompted us to record baseline locomotor activity in the mice by counting nocturnal infrared beam crossing events within a caged area over a period of 10 h. At 6 weeks and later, MeCP2 -/y mice became progressively lethargic when compared to wild-type littermates, and MeCP2 -/y animals treated with (1–3)IGF-1 showed a significant increase in activity levels compared to littermates treated with vehicle (Fig. 1*B*).

The impact of the drug on the lifespan and locomotor activity of the mutant mice was mirrored across other health measures characteristic of the disease. Abnormal breathing, another symptom of RTT (19, 33), was also impacted by the treatment. The change in mean breaths per minute was calculated to assess breathing variability (Fig. 1*C*). While Δ(breaths/minute) was significantly increased (implying greater variability) in MeCP2 -/y mice compared to wild-type littermates, Δ(breaths/minute) was significantly reduced (implying less variability) in MeCP2 -/y mice treated with (1–3)IGF-1.

Clinical evidence indicates that RTT patients suffer from reduced cardiac vagal tone that can cause life threatening cardiac arrhythmias (34). To examine heart rate abnormalities in MeCP2 -/y mice and the effect of (1–3)IGF-1 treatment, we monitored real time cardiac pulse rate in nonanesthetized wild-type and MeCP2 -/y animals treated with vehicle or (1–3)IGF-1 (Fig. 1*D*, see also Fig. S1). Wild-type mice exhibited a regular distribution of heart rate measurements centered near 750 beats per minute. In contrast, MeCP2 -/y mice exhibited a significantly lower average rate with substantial variability. Following treatment with (1–3)IGF-1, the variability was reduced while the average rate increased significantly. Together, these results show that (1–3)IGF-1 treatment significantly improves a range of physiological, behavioral, and autonomic parameters in MeCP2 mutant mice.

**Changes in Brain Structure in MeCP2 Mutant Mice and Effects of (1–3)IGF-1 Treatment.** A typical feature of RTT that is present in animal models of the disease is reduced brain weight (6). Since IGF1 is directly involved in development of brain size (35), we tested whether treatment with the active peptide positively affected brain weight in MeCP2 -/y animals (Fig. 2*A*). We confirmed that MeCP2 -/y mice had a significant reduction in brain weight compared to wild type. Importantly, (1–3)IGF-1 treatment significantly improved this feature in mutants.

We then asked whether MeCP2 mutant mice exhibited deficits in neurons and synapses of the brain consistent with a framework of altered synaptic maturation (12) and whether these changes could be impacted by treatment with (1–3)IGF-1. Since neurological correlates of physiological deficits are likely to be restricted to specific brain regions rather than the whole brain (3, 36), we focused our analysis on motor cortex in correspondence with the described motor phenotypes in MeCP2 mutant mice. To assess the status of synaptic development, we first measured the expression levels of PSD-95 by immunohistochemistry in layer 5 of motor cortex. PSD-95 is a key postsynaptic scaffold protein at excitatory synapses that directly promotes synapse maturation and exerts a major influence on synaptic strength and plasticity (37). We therefore examined whether PSD-95 levels were downregulated in adult MeCP2 mutant mice versus age-matched controls and whether PSD-95 levels could be increased via treatment with (1–3)IGF1 at the same age in which the locomotor activity phenotype was expressed. Motor cortex from MeCP2 mutant mice exhibited significantly less PSD-95 staining than the corresponding wild-type cortex, and treatment with (1–3)IGF-1 significantly increased PSD-95 levels (Fig. 2 *B* and *C*).

The number of excitatory synapses in the hippocampus has been reported to be significantly reduced in mice lacking MeCP2 (11, 13), although some reports do not observe changes in spine density (38). To approximate the number of excitatory synapses in our preparation, we used Golgi staining to label neurons sparsely and distinctly and visualized dendritic spine density on secondary dendritic branches of pyramidal neurons in layer 5 of motor cortex from adult mice. While low-magnification imaging clearly delineated the extent of the dendrites of these pyramidal cells (Fig. 2*D*), we could use higher magnifications to identify and count spines, the principal sites of excitatory synaptic contacts (Fig. 2*E*). Comparing the density of these spines per

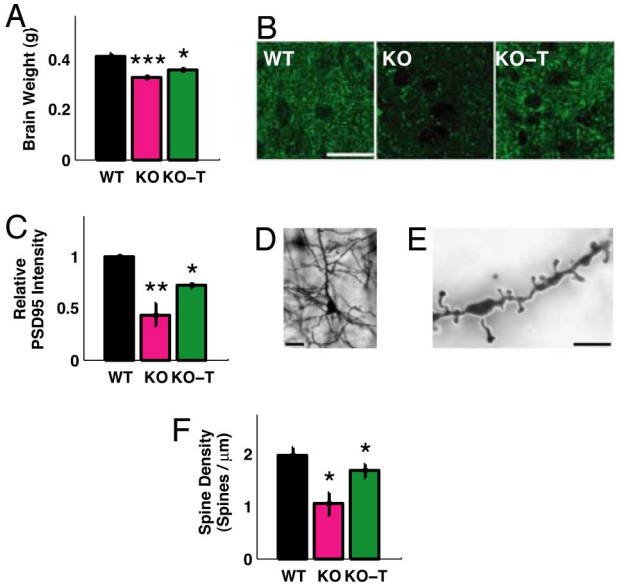


**Fig. 2.** Changes in brain structure in MeCP2 mutant mice and the effects of IGF-1 treatment. (*A*) Mean brain weight of P60 mice that were wild-type (WT), MeCP2 mutant (KO), or mutant treated with (1–3)IGF-1 (KO-T). MeCP2 mutant mice had reduced brain weight (WT, 0.41 ± 0.03 g, $n = 10$ mice; KO, 0.33 ± 0.02 g, $n = 8$ mice; $P < 0.0001$, two-tailed *t* test), and brain weight was elevated following treatment with (1–3)IGF-1 from approximately P15 onward (KO-T, 0.36 ± 0.02 g, $n = 10$ mice; KO vs. KO-T $P < 0.05$, two-tailed *t* test). ***: $P < 0.0001$; *: $P < 0.05$. (*B*) Immunostaining in motor cortex layer 5 for the synaptic scaffolding protein PSD-95 in wild-type mice (WT), untreated mutant mice (KO), and mutant mice treated with (1–3)IGF-1 (KO-T). (Scale bar: 25 μm.) (*C*) Quantitation of PSD-95 immunostaining depicting average labeling intensity normalized to wild-type intensity levels. Mutant animals (KO) exhibited significantly reduced levels of PSD-95 compared to wild-type (WT) (relative KO/WT expression level, 0.43 ± 0.11; $P < 0.01$, two-tailed *t* test, comparing WT and KO levels). Treatment with (1–3)IGF-1 (KO-T) increased PSD-95 levels significantly (KO-T/WT expression level, 0.70 ± 0.02; $P < 0.05$, two-tailed *t* test, comparing KO and KO-T levels). **: $P < 0.01$; *: $P < 0.05$. (*D*) Golgi staining of layer 5 pyramidal cells in adult motor cortex to enable specific, sparse labeling of neurons and spine morphology. (Scale bar: 25 μm.) (*E*) Imaging at higher magnification (100×) to enable clear identification of dendritic spines. (Scale bar: 1.25 μm.) (*F*) Spine density in adult (P60) animals is reduced in MeCP2 mutant mice and reversed by (1–3)IGF-1 treatment from P15 onward (WT, 1.98 ± 0.14 spines/μm, $n = 110$ spines, 6 cells, 2 mice; KO, 1.05 ± 0.22 spines/μm, $n = 133$ spines, 5 cells, 3 mice; KO-T, 1.68 ± 0.14 spines/μm, $n = 142$ spines, 7 cells, 3 mice; $P < 0.05$, two-tailed *t* test, comparing WT vs. KO and KO vs. KO-T). *: $P < 0.05$.

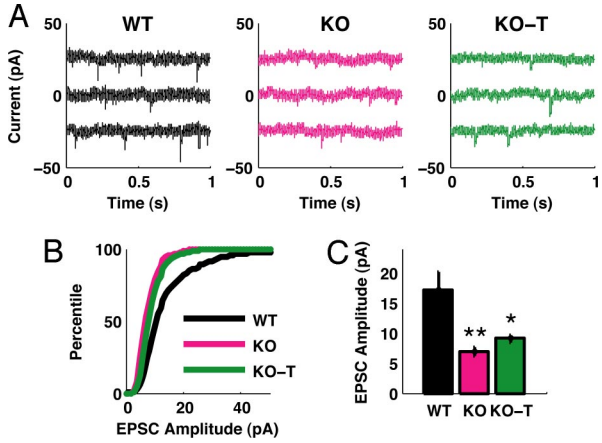


**Fig. 3.** Changes in synaptic transmission in MeCP2 mutant mice and the effects of IGF-1 treatment. (*A*) Representative traces from intracellular recordings of spontaneous excitatory postsynaptic currents (EPSCs) in acute slices from P28–32 sensorimotor cortex. Traces are presented for wild type (WT), mutant (KO), or mutant treated with (1–3)IGF-1 from P13–15 onward (KO-T). (*B*) Distributions of observed EPSC amplitudes measured across multiple cells, indicating a significant decrease in the size of EPSCs in mutant animals (WT, $n = 1543$ events, 11 cells; KO, 717 events, 6 cells, $P < 0.00001$ Kolmogorov-Smirnov test). Treatment with (1–3)IGF-1 partially but significantly reversed this trend (KO-T, $n = 1723$ events, 7 cells; KO-T vs. KO $P < 0.00001$ Kolmogorov-Smirnov test). (*C*) Mean EPSC amplitude, as in (*B*), for cells in each group. EPSCs are smaller in KO animals but larger with treatment of (1–3)IGF-1 (WT 17.3 ± 2.9 pA, KO 6.8 ± 0.8 pA, KO-T 9.1 ± 0.6 pA; WT vs. KO $P < 0.01$, KO vs. KO-T $P < 0.05$, two-tailed *t* test). **: $P < 0.01$; *: $P < 0.05$.

unit branch revealed a significant decrease in total spine density in neurons from mutant mice, a measure that was partially and significantly restored after treatment with (1–3)IGF-1 (Fig. 2*F*). Together these results demonstrate that lack of MeCP2 derails synaptic maturation in the motor cortex, and treatment with (1–3)IGF-1 seems to stimulate both the expression of synaptic scaffold protein and spine formation, leading to an increase in the number of spines on these neurons.

**Changes in Synaptic Transmission in MeCP2 Mutant Mice and Effects of (1–3)IGF-1 Treatment.** The morphological and molecular findings on synaptic structure in the pyramidal neurons of motor cortex suggested possible correlates in synaptic function that might be observed in the same cells of mutant and treated mice. Indeed, recent studies have reported that neurons across multiple brain regions of MeCP2 -/y mice display a profound reduction in spontaneous synaptic activity (13, 14, 18), a phenotype that is rescued by overexpression of BDNF (18). Similarly, acute application of an IGF-1 derivative has been shown to elevate evoked excitatory postsynaptic current (EPSC) amplitudes in rat hippocampal neurons in vitro (39). We thus reasoned that (1–3)IGF-1 application would augment functional excitatory transmission in MeCP2 mutant mice.

We acquired intracellular whole cell recordings from sensorimotor cortex in acute brain slices, measuring excitatory synaptic drive (spontaneous EPSC amplitude and frequency) in layer 5 cortical neurons of wild-type, MeCP2 mutant and treated animals (Fig. 3*A*). EPSCs recorded from MeCP2 -/y animals were significantly reduced in amplitude compared to EPSCs measured in wild-type animals (Fig. 3*B*). The trend was partially reversed in EPSCs recorded from MeCP2 -/y animals treated with (1–3)IGF-1, which were significantly larger in amplitude than EPSCs from MeCP2 -/y mice. These differences were also seen when averaging across cells (Fig. 3*C*). Measuring the distribution of time intervals between EPSC events also showed a slight increase in EPSC interval (reduced EPSC frequency) between wild-type and MeCP2 -/y animals (Fig. S2*A*), although this difference was not significant when mean EPSC interval was compared across cells (Fig. S2*B*), and there was no significant effect of the treatment in either measure. To evaluate whether our observed changes in spontaneous EPSC amplitude were influenced by changes in the intrinsic excitability of neurons, we injected current into cells and measured the frequency of evoked action potentials. We observed no significant difference in the I-V curves of the three treatment groups (Fig. S2*C*), suggesting that the observed changes in spontaneous EPSC amplitude arise from a synaptic mechanism. Quantifying the threshold for action potential in neurons from the 3 groups also yielded no significant difference (Fig. S2*D*).

Changes in spontaneous EPSC amplitude in MeCP2 mutant mice have been observed by others (13, 14), while a change in mEPSC frequency was observed in slices of hippocampus (13) but not cortex (14), and thus may be preparation-sensitive. Our findings indicate that the reduction of excitatory synaptic drive in sensorimotor cortical neurons of MeCP2 -/y mice, and its partial rescue following (1–3)IGF-1 treatment, are due at least

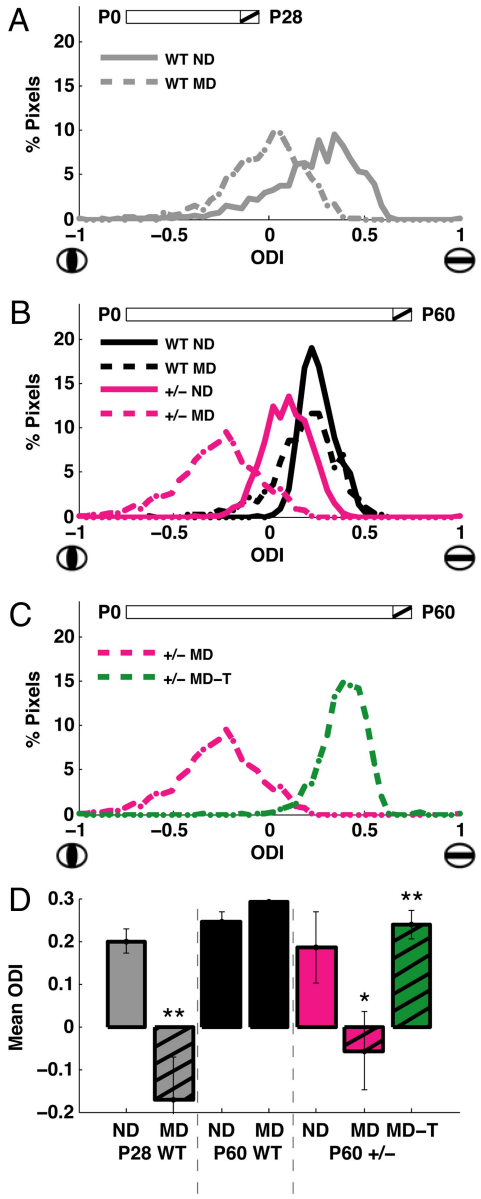


**Fig. 4.** Changes in cortical plasticity in MeCP2 mutant mice and the effects of IGF-1 treatment. (*A*) Ocular dominance index (ODI) scores observed for all pixels in visual cortex of two representative young (P28) wild-type animals, one of which was nondeprived (ND) and the other monocularly deprived (MD). Schematic at top depicts the 4 day period within the animal's lifespan at which deprivation occurred in the MD animal (hatched). Compared to the normal control (''WT ND,'' $n = 1071$ pixels), a population ODI shift was observed in the MD animal in favor of the open eye (''WT MD,'' $n = 1026$ pixels). (*D*) shows the comparison of ODI values across animals. (*B*) ODI scores from representative adult (P60) animals that were nondeprived (ND) or monocularly deprived (MD) for 4 days. In adult wild-type mice (black lines), a significant population ODI shift was not observed when comparing the monocularly deprived animal (''WT MD,'' $n = 1092$ pixels) to its nondeprived counterpart (''WT ND,'' $n = 2746$ pixels). In contrast, adult MeCP2+/− female mice (pink lines) did undergo a shift in population ODI following monocular deprivation (''+/- MD,'' $n = 2670$ pixels), compared to nondeprived mutants (''+/- ND,'' $n = 1484$ pixels) indicating that these adult mice exhibit similar cortical plasticity to the young mice depicted in *A*. (*D*) shows the comparison of ODI values across animals. (*C*) Pink line: adult MeCP2+/− female mouse that had undergone the MD-induced plasticity in ODI (''+/- MD''; same animal as in *B*). Green line: representative adult MeCP2+/− mouse that had been monocularly deprived for 4 days and treated with (1–3)IGF-1 (''+/- MD-T,'' $n = 3074$ pixels) from the first day of deprivation onward. Here the ODI of the treated mouse was significantly reversed from the mutant mouse, indicating that cortical plasticity had been abolished, preserving an ocular dominance profile typical of adult animals (as in *B*, ''WT ND'' or ''WT MD''). (*D*) shows the comparison of ODI values across animals. (*D*) Mean ODI values for developing wild-type mice (P28 WT, left), adult wild-type mice (P60 WT, middle), and adult MeCP2 deficient mice (P60 +/-, right). Positive ODI values indicate higher drive from the contralateral eye, and thus preserved organization, while reduced or negative values indicate higher drive from the ipsilateral eye, and thus altered circuitry. In young wild-type animals (gray bars, left), MD leads to a significant overall shift in ODI (*''ND'' 0.20 ± 0.02*, $n = 3$ animals; ''MD'' $-0.17 \pm 0.10$, $n = 4$ animals; $P < 0.01$, two-tailed $t$ test). In adult wild-type animals (black bars, middle), MD does not lead to a significant shift in ODI (*''ND'' 0.25 ± 0.02*, $n = 5$ animals; ''MD'' $0.29 \pm 0.04$, *$n = 5$ animals*). In adult MeCP2 deficient animals (pink bars, right), MD does shift ODI values significantly (*''ND'' 0.18 ± 0.08*, $n = 5$ animals; ''MD'' $-0.06 \pm 0.09$, $n = 5$ animals; $P < 0.05$, two-tailed $t$ test), as in the left gray bars. However, treatment with (1–3)IGF-1 from the first day of deprivation onward (green bar, right) prevents the shift in ODI (*''MD-T'' 0.24 ± 0.03*, $n = 5$ animals; $P < 0.01$, two-tailed $t$ test), such that responses are similar to wild-type adult animals. The MeCP2 deficient group only included female mice; the wild-type groups included both male and female mice since their ODI values were similar. **: $P < 0.01$; *: $P < 0.05$.

in part to changes in EPSC amplitude, providing a functional correlate to the structural changes in PSD-95 levels observed above.

**Changes in Cortical Plasticity in MeCP2 Mutant Mice and Effects of (1–3)IGF-1 Treatment.** We hypothesized that if the symptoms of RTT arise from prolonged immaturity of cortical synapses, an additional outcome would be that cortical circuitry in MeCP2 mutant mice would persist as more plastic or prone to change in response to alterations in inputs. We assessed the extent of cortical plasticity in vivo by measuring ''ocular dominance plasticity'' (40), a robust experimental paradigm for examining the maturation of visual cortex networks in which brief changes in visual drive produced by suturing one eye closed induce a functional reorganization of connections in the primary visual cortex, leading to a change in the relative responsiveness of cortical cells to stimulation of each eye (Fig. S3). In wild-type mice, these changes are only observed in circuits that are labile and not stable; thus, brief periods of monocular deprivation (MD) trigger ocular dominance plasticity in young but not adult animals.

We reasoned that if synaptic development was arrested in MeCP2-deficient mice, synapses in visual cortex of adult mice would still be sensitive to brief MD. To measure cortical responses elicited by stimulation of the eyes, we used optical imaging of intrinsic signals (*SI Methods*). Because adult MeCP2 mutant male mice develop severe symptoms at the age at which adult ocular dominance plasticity is typically assessed (around 8 weeks or later), we used MeCP2 heterozygous females, which develop milder symptoms but are considered an accurate model for RTT (41, 42).

We first performed optical imaging in young, nondeprived wild-type mice (aged postnatal day 28) and plotted the ocular dominance values ($-1$, ipsilateral eye dominated, to $+1$, contralateral eye dominated) for the distribution of pixels across the cortical surface (Fig. 4*A*). In age-matched wild-type animals that had undergone 4 days of MD, this distribution was seen to shift noticeably away from the closed eye in favor of the open eye. In contrast, the MD paradigm in adult wild-type mice (aged P60, Fig. 4*B*, black traces) failed to produce a shift in the ocular dominance distribution when compared to nondeprived mice. Age-matched MeCP2+/− female mice however showed a significant shift in the visually driven response in favor of the open eye after 4 days of MD (Fig. 4*B*, pink traces). Such persistence of rapid ocular dominance plasticity in the visual cortex following unbalanced visual drive is a feature that is typical of an immature cortex (Fig. 4*A*) and is consistent with a deficit in synaptic maturation or stabilization that persists into adulthood following MeCP2 deficiency.

Treatment with (1–3)IGF-1 prevents ocular dominance plasticity in wild-type young mice (22), and direct infusion of IGF-1 into the visual cortex of immature rats stimulates the activity-dependent maturation of cortical circuitry (43). We therefore tested if (1–3)IGF-1 treatment could stabilize the prolonged ocular dominance plasticity observed in adult MeCP2+/− mice. Indeed, P60 mice that underwent MD while being administered (1–3)IGF-1 failed to show an ocular dominance shift, with a distribution that was significantly reversed from the untreated animals (Fig. 4*C*).

These findings were observed across all animals (Fig. 4*D*). In contrast to the effect of MD in young wild-type (P28 WT) mice, ocular dominance plasticity was not observed in adult wild-type (P60 WT) mice. However, ocular dominance plasticity was again observed in adult MeCP2 (P60 +/−) mice, a feature that was not seen following treatment with (1–3)IGF-1. Thus, strikingly, treatment with (1–3)IGF-1 abolishes the plasticity observed in the adult MeCP2 deficient mice, allowing stable representations to persist as in the adult wild-type mice.

## Discussion

Mutation in the gene encoding MECP2 have been shown to cause RTT in girls and congenital encephalophathy in boys (42). Mouse models with different mutations in the MeCP2 gene all show symptoms that are characteristic of the disease (6–8), although the severity of the phenotype relates to the kind of mutation (44). In this study, we have examined MeCP2 mutant mice with an in-frame deletion of exon 3 (6), and we provide evidence that (1–3)IGF-1 ameliorates symptoms of RTT in these mice. Specifically, we show that (1–3)IGF-1 treatment leads to a partial rescue of nine separate measures of organismal function, as well as brain structure and function: (*i*) lifespan, (*ii*) locomotor activity, (*iii*) respiratory function, (*iv*) heart rate, (*v*) brain weight, (*vi*) concentration of a postsynaptic density protein in motor cortex, (*vii*) spine density on motor cortex neurons, (*viii*) excitatory synaptic transmission in sensorimotor cortex neurons, and (*ix*) cortical circuit plasticity.

Mechanistically, our data fit the hypothesis that loss of MeCP2 leads to an inability of synapses and the circuits they comprise to mature, at least in specific cortical regions, and treatment with (1–3)IGF-1 partially reverses this deficit. Several lines of evidence support the suggestion that synapses in MeCP2 deficient mice are immature compared to wild-type animals and that immature synapses and circuits persist into adulthood in MeCP2 deficient mice. First, PSD-95, a postsynaptic density scaffold protein that enhances synapses maturation and stabilization (37), is down-regulated in motor cortex of MeCP2 mutant mice, and the number of synaptic contacts is reduced as well (Fig. 2). Second, single neurons exhibit a reduction in amplitude of excitatory postsynaptic currents such that overall synaptic transmission is weaker (Fig. 3). Third, visual cortex connections in adult MeCP2 deficient mice display features of plasticity following monocular deprivation usually characteristic of young mice (Fig. 4). Systemic treatment of MeCP2 mutant mice with (1–3)IGF-1 results in substantial improvement across the spectrum of these metrics. Indeed, the abnormalities in respiration and heart rate in MeCP2 mutant mice can also be attributed to deficits in maturation of brainstem regulatory systems (19). Consistent with this hypothesis, (1–3)IGF-1 improves respiration and cardiac abnormalities, in addition to improvements in locomotor activity and lifespan that are observed in the mutant mice (Fig. 1).

Although the levels of IGF-1 in serum or cerebrospinal fluid may not be significantly reduced in RTT patients (45), we posit that stimulation of the IGF-1 signaling pathway can impact synaptic maturation and function and can do so via multiple mechanisms. PSD-95 may be activated directly via known intermediaries of the IGF-1 pathway, PI3K and pAkt (22, 24). Interestingly, this same pathway is prominently stimulated by BDNF (23), which is known to be effective in reversing RTT phenotypes (18). (1–3)IGF-1 treatment phosphorylates the IGF-1 receptor and also leads to activation of the MAPK cascade (data not shown), another signaling pathway that is stimulated by BDNF and is involved in synaptic stabilization (17, 46). Although IGF-1 treatment does not increase BDNF levels in MeCP2 mutant mice (as measured with ELISA on whole brain extracts of MeCP2 -/y adult mice, data not shown), it is plausible that it would partially mimic BDNF action by stimulating common downstream signals (23, 46). IGF-1 infusion into the brain up-regulates intracortical inhibition and the expression of extracellular matrix molecules (43), which are additional mechanisms that promote the maturation and stabilization of cortical circuits (47). IGF-1 deficient mice show a reduction in the number of parvalbuminergic neurons (35). Consistent with these observations, we find a reduction of GABA immunostained neurons in MeCP2 -/y mice and a marked increase in treated mice (Fig. S4). Finally, IGF-1 is one of the signals that is up-regulated by environmental enrichment (43), a rearing condition which also ameliorates motor coordination symptoms in MeCP2 mutant mice (48).

While the multiple restorative effects that we observe in the mutant mice following treatment are highly significant individually and in concert, it is important to stress that MeCP2 mutant mice treated with (1–3)IGF-1 still develop the full range of symptoms and die prematurely. Moreover, we cannot exclude the possibility that (1–3)IGF-1 affects nonneuronal cells; for example (1–3)IGF-1 treatment could increase vascular density and glucose utilization in the brain or have additional effects in peripheral tissues (49). In the experiments described, (1–3)IGF-1 was administered to the mice via i.p. injections. It is possible that other delivery methods, such as i.v. infusion or ventricular delivery would be more effective and potentially could further improve the extent of rescue of the symptoms.

In conclusion, we have shown that systemic delivery of (1–3)IGF-1 can significantly improve physiological behavior and survival in MeCP2 mutant mice. We also provide direct evidence that MeCP2 deficiency leads to immature synaptic function and organization in a manner that can be partially rescued by (1–3)IGF-1 administration. While further studies will be needed to unravel the exact mechanism of IGF-1 action, the results presented here point to a potential utility of full-length IGF-1 or its derivatives in the treatment of RTT. Such prospective therapies also have significant implications for other autism spectrum disorders and neurodevelopmental conditions that have similar phenotypes, genetic susceptibility, and underlying neurobiological mechanisms.

## Materials and Methods

**Mice.** The MeCP2 germline null allele from Chen, *et al.* (6) was used. Genotyping was performed as described (6). All experiments were performed according to protocols approved by the Animal Care and Use Committee at Massachusetts Institute of Technology and conformed to National Institutes of Health guidelines.

**(1–3)IGF-1 Treatment.** (1–3)IGF-1 is the N-terminal tri-peptide of IGF-1 (Bachem Biosciences). Detailed information on doses is provided in *SI Methods*.

**Nocturnal Activity, Breath Rate, and Heart Rate Measurements.** Spontaneous motor activity was measured as described in (6). Real time blood oxygenation and cardiac pulse were measured together using a tail clip sensor (Mouse OX Oximeter). For details see *SI Methods*.

**Immunohistochemistry and Golgi Staining.** Sections were prepared and processed according to (22). Details are provided in *SI Methods*. For Golgi staining, adult mice from different experimental groups were transcardially perfused with saline and brains extracted. Brains were processed with FD Rapid Golgi Staining Kit (FD Neurotechnologies) according to the manufacturer's instructions. Sections from these samples were cut at 250 $\mu$m thickness and mounted onto slides, then developed according to the user's manual. Images were

acquired at 10× (whole cell) and 200× (spine imaging) using a Zeiss transmitted light microscope.

**Slice Physiology and Optical Imaging of Intrinsic Signals.** Slice physiology preparation and whole cell recordings were performed as described in *SI Methods*. Methods for animal preparation for optical imaging and for data acquisition and analysis were as described (22).

**Statistical Treatment and Analysis.** All statistically significant P-values reported in 3-bar histograms were verified first via ANOVA and then paired two-tailed t-tests. All error bars represent standard errors of the mean.

**ACKNOWLEDGMENTS.** We thank Orsolya Kuti and Jessie Dausmann for excellent technical assistance, and Sam H. Horng and Shomit Sengupta for useful scientific discussion and critical reading of the manuscript. We thank Morgan Sheng and Martha Constantin-Paton for discussion regarding PSD-95 detection and immunostaining. We also thank George Bell for help with statistical analysis and Tom di Cesare for graphics support. This work was supported by Ruth Kirschstein National Research Service Award postdoctoral fellowships (F32-EYO17240 and F32-EY017500, National Institutes of Health) to DT and NRW, a predoctoral fellowship from the Boehringer Ingelheim foundation to EG, grants from the Rett Syndrome Research Foundation and National Institutes of Health (R01-CA087869 and R01-HD045022) to RJ, and grants from the Simons Foundation, the Marcus Family Foundation, and the Autism Consortium to MS.

1. Chahrour M, Zoghbi HY (2007) The story of rett syndrome: From clinic to neurobiology. *Neuron* 56:422–437.
2. Amir RE, *et al.* (1999) Rett syndrome is caused by mutations in X-linked MECP2, encoding methyl-CpG-binding protein 2. *Nat Genet* 23:185–188.
3. Chahrour M, *et al.* (2008) MeCP2, a key contributor to neurological disease, activates and represses transcription. *Science* 320:1224–1229.
4. Nan X, *et al.* (1998) Transcriptional repression by the methyl-CpG-binding protein MeCP2 involves a histone deacetylase complex. *Nature* 393:386–389.
5. Cohen DR, *et al.* (2003) Expression of MeCP2 in olfactory receptor neurons is developmentally regulated and occurs before synaptogenesis. *Mol Cell Neurosci* 22:417–429.
6. Chen RZ, Akbarian S, Tudor M, Jaenisch R (2001) Deficiency of methyl-CpG binding protein-2 in CNS neurons results in a Rett-like phenotype in mice. *Nat Genet* 27:327–331.
7. Guy J, Hendrich B, Holmes M, Martin JE, Bird A (2001) A mouse Mecp2-null mutation causes neurological symptoms that mimic Rett syndrome. *Nat Genet* 27:322–326.
8. Shahbazian M, *et al.* (2002) Mice with truncated MeCP2 recapitulate many Rett syndrome features and display hyperacetylation of histone H3. *Neuron* 35:243–254.
9. Guy J, Gan J, Selfridge J, Cobb S, Bird A (2007) Reversal of neurological defects in a mouse model of Rett syndrome. *Science* 315:1143–1147.
10. Giacometti E, Luikenhuis S, Beard C, Jaenisch R (2007) Partial rescue of MeCP2 deficiency by postnatal activation of MeCP2. *Proc Natl Acad Sci USA* 104:1931–1936.
11. Smrt RD, *et al.* (2007) Mecp2 deficiency leads to delayed maturation and altered gene expression in hippocampal neurons. *Neurobiol Dis* 27:77–89.
12. Johnston MV, Jeon OH, Pevsner J, Blue ME, Naidu S (2001) Neurobiology of Rett syndrome: A genetic disorder of synapse development. *Brain Dev* 23 *Suppl* 1:S206–S213.
13. Chao HT, Zoghbi HY, Rosenmund C (2007) MeCP2 controls excitatory synaptic strength by regulating glutamatergic synapse number. *Neuron* 56:58–65.
14. Dani VS, *et al.* (2005) Reduced cortical activity due to a shift in the balance between excitation and inhibition in a mouse model of Rett syndrome. *Proc Natl Acad Sci USA* 102:12560–12565.
15. Tudor M, Akbarian S, Chen RZ, Jaenisch R (2002) Transcriptional profiling of a mouse model for Rett syndrome reveals subtle transcriptional changes in the brain. *Proc Natl Acad Sci USA* 99:15536–15541.
16. Chen WG, *et al.* (2003) Derepression of BDNF transcription involves calcium-dependent phosphorylation of MeCP2. *Science* 302:885–889.
17. Carvalho AL, Caldeira MV, Santos SD, Duarte CB (2008) Role of the brain-derived neurotrophic factor at glutamatergic synapses. *Br J Pharmacol* 153 *Suppl* 1:S310–324.
18. Chang Q, Khare G, Dani V, Nelson S, Jaenisch R (2006) The disease progression of Mecp2 mutant mice is affected by the level of BDNF expression. *Neuron* 49:341–348.
19. Ogier M, *et al.* (2007) Brain-derived neurotrophic factor expression and respiratory function improve after ampakine treatment in a mouse model of Rett syndrome. *J Neurosci* 27:10912–10917.
20. D'Ercole AJ, Ye P, Calikoglu AS, Gutierrez-Ospina G (1996) The role of the insulin-like growth factors in the central nervous system. *Mol Neurobiol* 13:227–255.
21. O'Kusky JR, Ye P, D'Ercole AJ (2000) Insulin-like growth factor-I promotes neurogenesis and synaptogenesis in the hippocampal dentate gyrus during postnatal development. *J Neurosci* 20:8435–8442.
22. Tropea D, *et al.* (2006) Gene expression changes and molecular pathways mediating activity-dependent plasticity in visual cortex. *Nat Neurosci* 9:660–668.
23. Yoshii A, Constantine-Paton M (2007) BDNF induces transport of PSD-95 to dendrites through PI3K-AKT signaling after NMDA receptor activation. *Nat Neurosci* 10:702–711.
24. Zheng WH, Quirion R (2004) Comparative signaling pathways of insulin-like growth factor-1 and brain-derived neurotrophic factor in hippocampal neurons and the role of the PI3 kinase pathway in cell survival. *J Neurochem* 89:844–852.
25. Ramsey MM, Adams MM, Ariwodola OJ, Sonntag WE, Weiner JL (2005) Functional characterization of des-IGF-1 action at excitatory synapses in the CA1 region of rat hippocampus. *J Neurophysiol* 94:247–254.
26. Chang YS, *et al.* (2004) Mechanisms underlying lack of insulin-like growth factor-binding protein-3 expression in non-small-cell lung cancer. *Oncogene* 23:6569–6580.
27. Itoh M, *et al.* (2007) Methyl CpG-binding protein 2 (a mutation of which causes Rett syndrome) directly regulates insulin-like growth factor binding protein 3 in mouse and human brains. *J Neuropathol Exp Neurol* 66:117–123.
28. Riikonen R, *et al.* (2006) Cerebrospinal fluid insulin-like growth factors IGF-1 and IGF-2 in infantile autism. *Dev Med Child Neurol* 48:751–755.
29. Baker AM, *et al.* (2005) Central penetration and stability of N-terminal tripeptide of insulin-like growth factor-I, glycine-proline-glutamate in adult rat. *Neuropeptides* 39:81–87.
30. Guan J, *et al.* (2004) Neuroprotective effects of the N-terminal tripeptide of insulin-like growth factor-1, glycine-proline-glutamate (GPE) following intravenous infusion in hypoxic-ischemic adult rats. *Neuropharmacology* 47:892–903.
31. Sizonenko SV, Sirimanne ES, Williams CE, Gluckman PD (2001) Neuroprotective effects of the N-terminal tripeptide of IGF-1, glycine-proline-glutamate, in the immature rat brain after hypoxic-ischemic injury. *Brain Res* 922:42–50.
32. Kaufmann WE, Taylor CV, Hohmann CF, Sanwal IB, Naidu S (1997) Abnormalities in neuronal maturation in Rett syndrome neocortex: Preliminary molecular correlates. *Eur Child Adolesc Psychiatry* 6 *Suppl* 1:75–77.
33. Julu PO, *et al.* (2008) Cardiorespiratory challenges in Rett's syndrome. *Lancet* 371:1981–1983.
34. Julu PO, *et al.* (2001) Characterisation of breathing and associated central autonomic dysfunction in the Rett disorder. *Arch Dis Child* 85:29–37.
35. Beck KD, Powell-Braxton L, Widmer HR, Valverde J, Hefti F (1995) Igf1 gene disruption results in reduced brain size, CNS hypomyelination, and loss of hippocampal granule and striatal parvalbumin-containing neurons. *Neuron* 14:717–730.
36. Fyffe SL, *et al.* (2008) Deletion of Mecp2 in Sim1-expressing neurons reveals a critical role for MeCP2 in feeding behavior, aggression, and the response to stress. *Neuron* 59:947–958.
37. El-Husseini AE, Schnell E, Chetkovich DM, Nicoll RA, Bredt DS (2000) PSD-95 involvement in maturation of excitatory synapses. *Science* 290:1364–1368.
38. Moretti P, *et al.* (2006) Learning and memory and synaptic plasticity are impaired in a mouse model of Rett syndrome. *J Neurosci* 26:319–327.
39. Xing C, *et al.* (2007) Effects of insulin-like growth factor 1 on synaptic excitability in cultured rat hippocampal neurons. *Exp Neurol* 205:222–229.
40. Berardi N, Pizzorusso T, Ratto GM, Maffei L (2003) Molecular basis of plasticity in the visual cortex. *Trends Neurosci* 26:369–378.
41. Stearns NA, *et al.* (2007) Behavioral and anatomical abnormalities in Mecp2 mutant mice: A model for Rett syndrome. *Neuroscience* 146:907–921.
42. Schule B, Armstrong DD, Vogel H, Oviedo A, Francke U (2008) Severe congenital encephalopathy caused by MECP2 null mutations in males: Central hypoxia and reduced neuronal dendritic structure. *Clin Genet* 74:116–126.
43. Ciucci F, *et al.* (2007) Insulin-like growth factor 1 (IGF-1) mediates the effects of enriched environment (EE) on visual cortical development. *PLoS ONE* 2:e475.
44. Belichenko NP, Belichenko PV, Li HH, Mobley WC, Francke U (2008) Comparative study of brain morphology in Mecp2 mutant mouse models of Rett syndrome. *J Comp Neurol* 508:184–195.
45. Vanhala R, Turpeinen U, Riikonen PR (2000) Insulin-like growth factor-I in cerebrospinal fluid and serum in Rett syndrome. *J Child Neurol* 15:797–802.
46. Thomas GM, Huganir RL (2004) MAPK cascade signalling and synaptic plasticity. *Nat Rev Neurosci* 5:173–183.
47. Tropea D, Van Wart A, Sur M (2008) Review. Molecular mechanisms of experience-dependent plasticity in visual cortex. *Philos Trans R Soc Lond B* 364:341-355.
48. Kondo M, *et al.* (2008) Environmental enrichment ameliorates a motor coordination deficit in a mouse model of Rett syndrome–Mecp2 gene dosage effects and BDNF expression. *Eur J Neurosci* 27:3342–3350.
49. Sonntag WE, Ramsey M, Carter CS (2005) Growth hormone and insulin-like growth factor-1 (IGF-1) and their influence on cognitive aging. *Ageing Res Rev* 4:195–212.